Journal of Transportation Technologies, 2026, 16(1), 38-53
https://www.scirp.org/journal/jtts
ISSN Online: 2160-0481
ISSN Print: 2160-0473

Development of a Platform for Real-Time, Non-Disruptive Monitoring and Early Fault Detection of Critical High Voltage Transformers and Switchgears in High Speed-Rail

Ming Zhu[1], Jiawei Fan[1], Yingtao Jiang[1], Hualiang Teng[2]

[1]Department of Electrical and Computer Engineering, University of Nevada Las Vegas, Las Vegas, USA
[2]Department of Civil and Environmental Engineering and Construction, University of Nevada Las Vegas, Las Vegas, USA
Email: ming.zhu@unlv.edu, yingtao.jiang@unlv.edu, Hualiang.teng@unlv.edu

How to cite this paper: Zhu, M., Fan, J.W., Jiang, Y.T. and Teng, H.L. (2026) Development of a Platform for Real-Time, Non-Disruptive Monitoring and Early Fault Detection of Critical High Voltage Transformers and Switchgears in High Speed-Rail. *Journal of Transportation Technologies*, **16**, 38-53.
https://doi.org/10.4236/jtts.2026.161003

Received: October 8, 2025
Accepted: December 5, 2025
Published: December 8, 2025

Abstract

Partial discharge (PD) incidents in high-speed rail systems, such as transformers and switchgears, arise from insulation defects under electric stress, leading to potential flashovers, breakdowns, downtime, and safety risks. PD emits radio frequency (RF) signals, enabling the development of a non-invasive, real-time PD detection and monitoring platform. This system uses an RF antenna and a high-speed data acquisition system to scan a frequency range (100 MHz to 2.5 GHz) with intermediate frequency modulation for precise detection and analysis. PD events exceeding a preset power threshold are recorded, capturing both signal data and spectrum snapshots. Real-time data is streamed to a cloud server, accessible via a smartphone app, allowing remote monitoring and quick responses by maintenance teams. Laboratory tests confirm the system's effectiveness in accurately capturing PD signals, enhancing high-speed rail infrastructure reliability and safety.

Keywords

Partial Discharge, Real-Time Monitoring, Robust Detection, Radio Frequency

1. Introduction

High-speed rail (HSR) has revolutionized transportation since 1960 by providing rapid, efficient, and reliable services that connect major cities and regions [1]. Extensive HSR networks have been developed in numerous countries, including Japan, France, Germany, China [2], and the undergoing California High-Speed Rail

(CAHSR) project from Sacramento/San Francisco Bay Area to the Greater Los Angeles/San Deigo [3], showcasing significant advancements in speed, safety, and passenger comfort.

The efficient and reliable operation of high-speed rail systems relies heavily on sophisticated high-voltage electrical facilities, such as transformers and switchgears, to ensure the seamless transmission and distribution of electrical power for train operations [4]-[6]. However, these high-voltage assets are susceptible to partial discharge (PD), which occurs when the electric field intensity exceeds the dielectric strength of the insulating material, causing localized discharges that do not completely bridge the insulation. These discharges typically result from defects such as voids, cracks, or contaminants within the insulation, which can arise during manufacturing, installation, or due to aging and environmental factors [7]. The occurrence of PD in high-voltage transformers and switchgears can have severe consequences, such as generating heat and chemical byproducts that degrade the insulating material over time. This degradation leads to erosion, cracks and carbonization, progressively weakening the insulation's ability to withstand high voltages (**Figure 1**). Such phenomenon may significantly undermine the performance and longevity of transformers and switchgears, resulting in costly repairs, down time and/or fire hazards [8] [9]. According to the research [10] [11], 85% of high-voltage facility failures and asset damages are due to the PD activities (**Figure 2**).

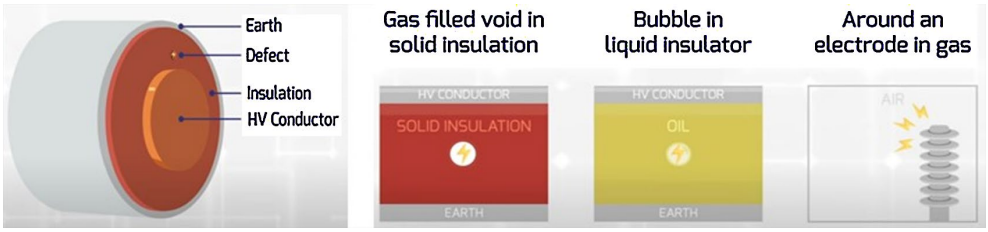

Figure 1. Causes of PD in switchgears and transformers.

To mitigate the risks associated with PD, it is crucial to implement effective monitoring and maintenance strategies. There are multiple approaches to detect PD, such as electromagnetic method [12]-[14], electrical method [15]-[18], chemical [19]-[22], acoustic [23]-[25], optical [26] [27] and combinations of these methods [28]-[31]. However, electrical and chemical methods require contact with the equipment, which may bring interference of normal railway operations; whereas acoustic and optical methods may be disrupted by the environmental noises that may affect the detection accuracy.

On the other hand, since PD usually emits a radio frequency (RF) signal in a range between 300 and 1500 MHz, we can employ one or multiple ultra-high-frequency (UHF) antenna(s) to scan and detect RF signals in the air within this spectrum. However, continuously and losslessly monitoring PD signals that span over a wide frequency range of up to 1500 MHz usually requires a minimum sampling rate of 3GHz (*i.e.*, 3×10^9 samples per second) of the data acquisition

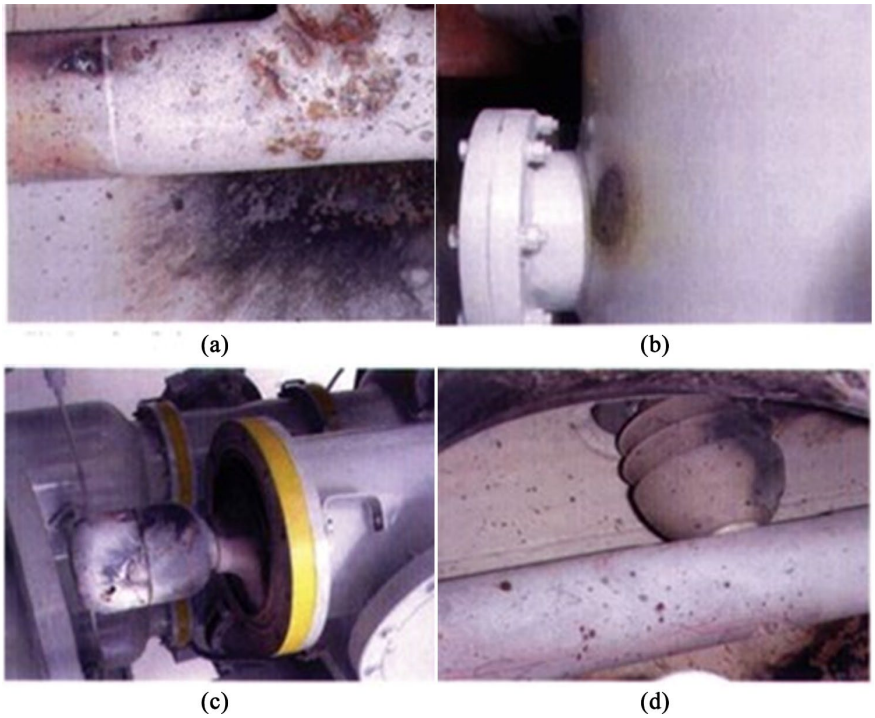

Figure 2. Damages caused by PD hazards. (a) Inner surface burn; (b) Burn through the shield; (c) Contact damage; (d) Explosion of the pillar insulator.

system (DAS), proposing an excessive hardware challenge in processing this huge amount of data. Developing such high-speed customized DAS is often costly and takes a long time to align all hardware to work effectively and reliably. In addition, a single UHF antenna may not suffice the demand to constantly capture PD signals of such broadband, and employing multiple antennas will bring extra complexity to the circuit.

To resolve such challenges, we propose to use a single antenna to iteratively scan the spectrum from 100 MHz to 2500 MHz with intermediate frequency (IF) modulation [32] [33]. In this way, the system only has one input and is flexible to various scanning spectrums by adjusting the IF modulation frequencies. One drawback of this method is that the band-limited antenna can only scan a small range of RF spectrum at a time while leaving other spectrum unattended, causing the possibility of missing the PD. Nevertheless, as long as the PD events are repetitive and with proper configuration of the scanning rate, the system will catch PD occurrence confidently.

The organization of this paper is as follows. The development of the proposed PD detection and cloud-based monitoring is described in Section 2, and the system evaluations are illustrated in Section 3. The conclusion is drawn in Section 4.

2. Development of a Non-Disruptive Real-Time PD Detection and Monitoring System

This chapter introduces the developed hardware and software platform for PD signal capturing, detection and recording, as well as the cloud-based remote access

on the smartphone (Figure 3). The PD signal data acquisition system only consists of an antenna with a passing bandwidth of 800 MHz centered at 136 MHz, a Tektronix RSA 306B real-time RF spectrum analyzer [34], and a computer (or other high-performance embedded system) with USB-3 interface. Key specifications of the RSA 306B are listed in Table 1.

Figure 3. IoT-cloud-based remote accessible real-time PD monitoring system diagram.

Table 1. Key specification of tektronix RSA 306b real-time RF analyzer.

Detection Frequency	9 K - 6.2 GHz
Sampling Frequency	112 MSa/s
IF Bandwidth	Max. 40 MHz
ADC bit-width	14-bit
Amplitude Accuracy	About 1 dB
Max DC Level	±40 Vdc
Average Noise	≤−130 dB

2.1. PD Data Acquisition Process

During each PD sampling process, the RF antenna contactlessly senses the PD signals in the air and conveys them to the RSA 306B, which sets up an intermediate frequency (IF) carrier signal to shift the ultra-high frequency PD signals to a lower spectrum (*i.e.*, IF modulation). The modulated signal will then be sampled, quantified and digitized by high-speed analog-to-digital converter (ADC), and the data stream will be transmitted to the computer via USB-3 connection (Figure 4). Here, we call the data within one sample duration (*i.e.*, 10 milliseconds in this study) a data or sample frame. The computer reads the data frame via Tektronix application programing interface (API) [35], and calculates the data in both time domain in-phase/quadrature (I/Q) stream form (*i.e.*, quadrature modulation) (Figure 5) [36] and spectrum form (Figure 6) using Fourier Transform, Equation

(1). The power is calculated as Equation (2).

$$X[k]=\sum_{n=0}^{N-1}x(n)e^{-j2\pi kn/N} \tag{1}$$

$$Power=10\log\left(\frac{I^2+Q^2}{1mW}\right) \tag{2}$$

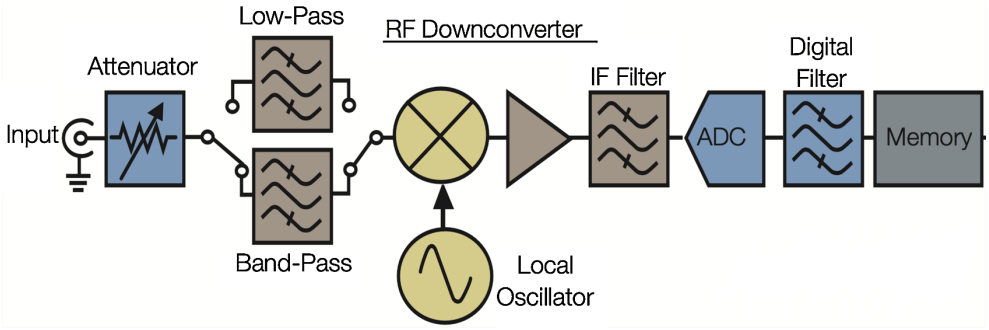

Figure 4. Signal capturing, modulation and sampling in RSA 306B.

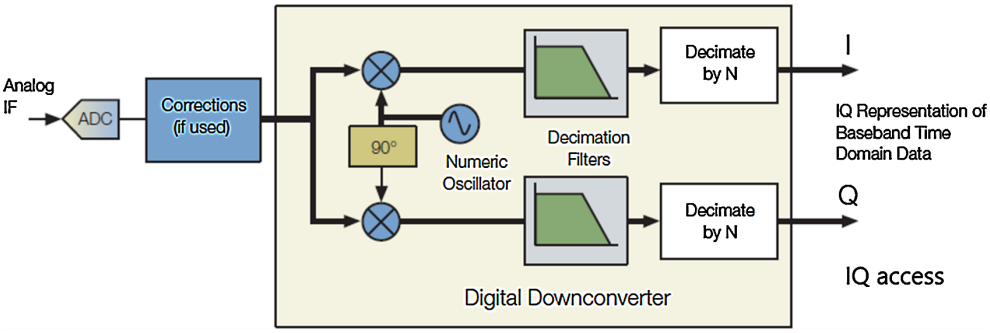

Figure 5. I/Q modulation for data in time domain [36].

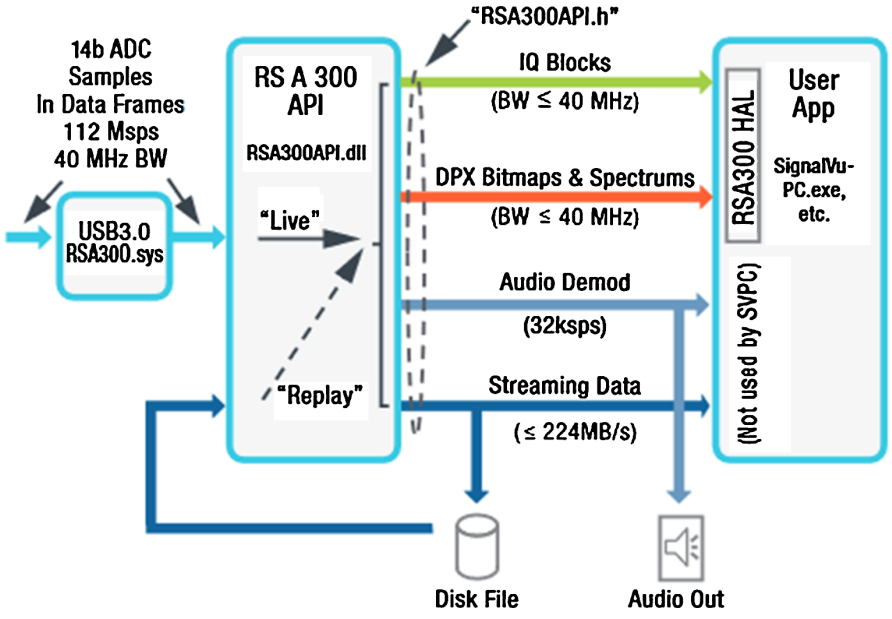

Figure 6. RSA API and data flow in computer [36].

If the system detects any signal power exceeding a pre-set threshold (*i.e.*, −50 dB in this study) during each sample frame, the I/Q data and spectrum information of that frame will be recorded in .r3f and siq format (Figure 7), which can be further decoded to the time sequence .csv files. The fundamental functions of data acquisition are fulfilled by C/C++ based on RSA 306B API, and a python interface is implemented on top of the C/C++ code and RSA API for the simplicity of user interaction and process control.

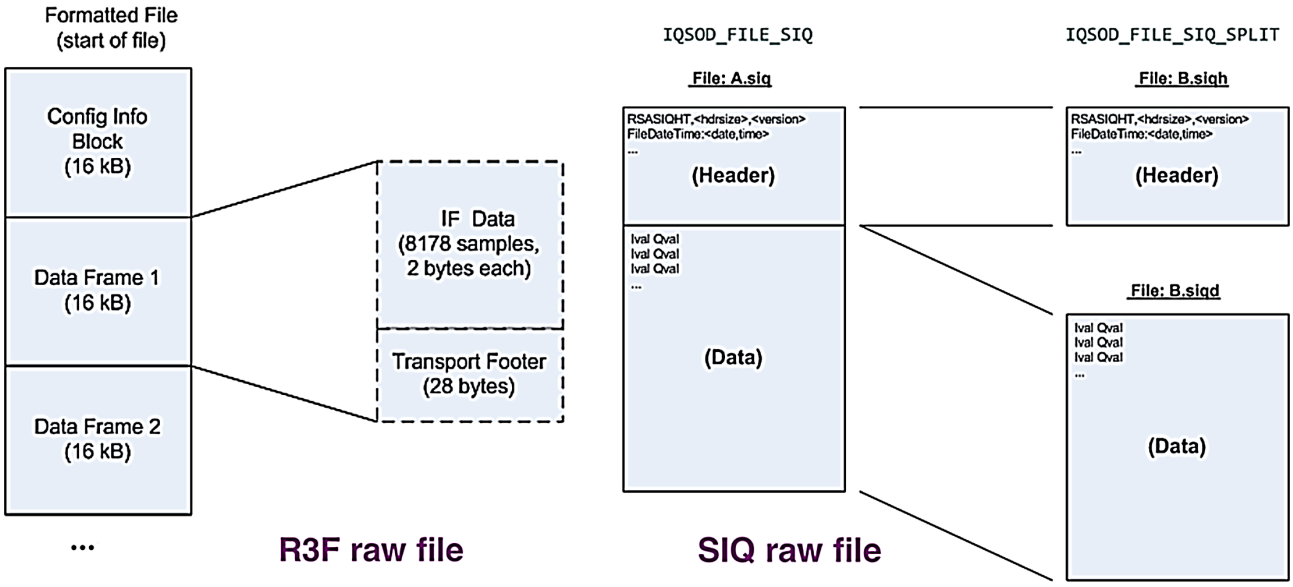

Figure 7. r3f and .siq file for data storage [36].

As the RSA has the sampling rate of 112 MHz and its signal sampling bandwidth of 40 MHz, for each complete PD scanning process, the system will iteratively set RSA's IF modulation carrier frequency from 100 MHz to 2500 MHz (*i.e.*, one iteration), with an incremental step of 40 MHz, to cover the PD signal frequency of interest (Figure 8). In the end of each iteration (*i.e.*, 61 samples in 60 iterations of 600 milli-seconds), the system will stitch the power-spectrum diagram of each sample frame for a complete diagram, and remove I/Q data that does not include any PD signals. If any PD signals are captured, the corresponding I/Q data and power-spectrum diagrams will be kept and named according to the timestamp and detected PD frequency. In this way, users can easily observe and trace back the records of PD occurrences, and the system storage can be more efficiently utilized.

2.2. Remote Access to Continuous Real-Time PD Monitoring

With the expansion of widely spread high-speed rail network, internet of things (IoT) technology should be added to local PD detection and monitoring system at each switchgear/transformer station for the remote accessibility and potentially instant responsiveness to any alert messages it may generate. To achieve this goal, the google cloud service (e.g., Google Drive, Firebase, etc.) is employed and a

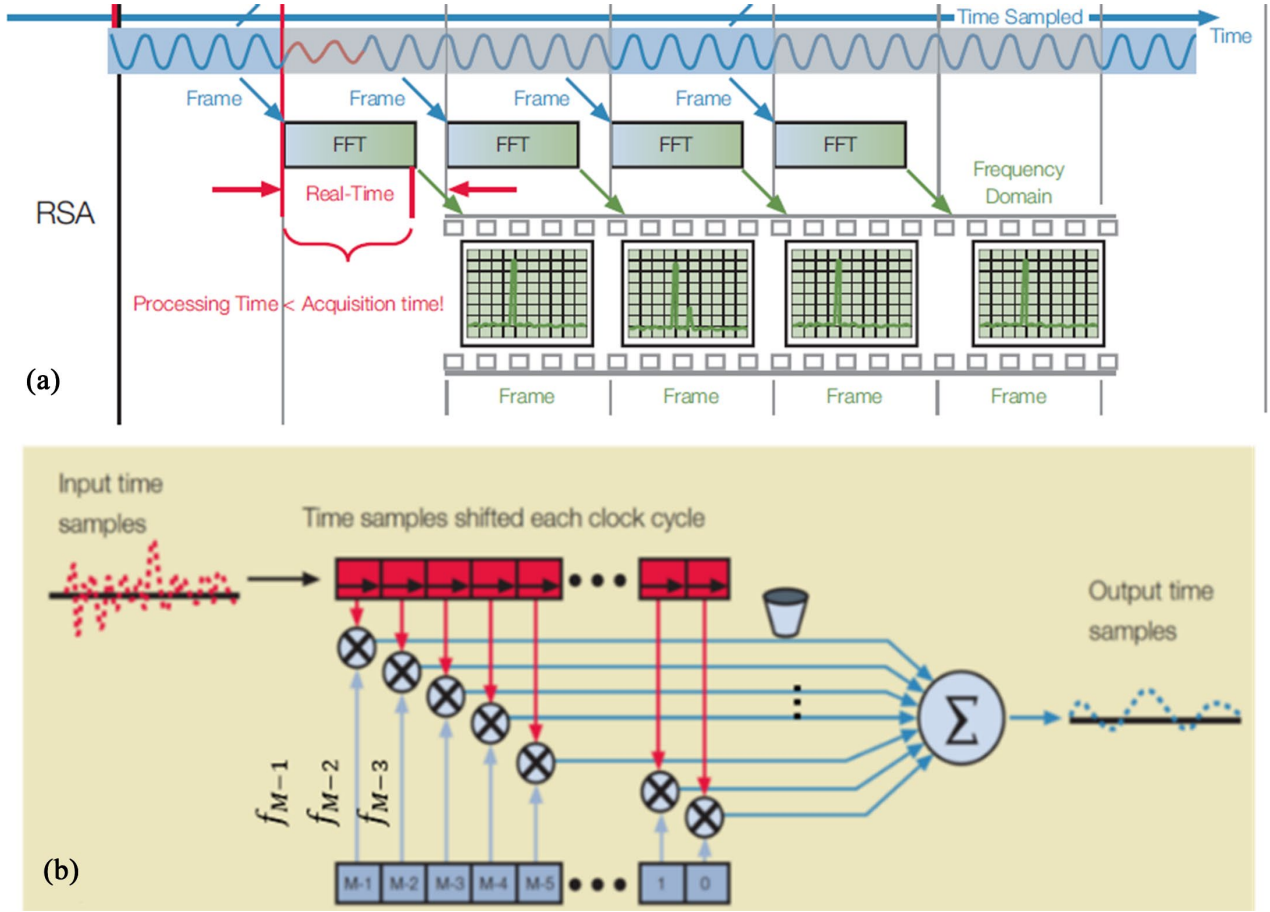

Figure 8. (a) Iterative sampling and spectrum analysis; (b) Iterative scanning to cover the entire PD spectrum.

smartphone application (APP) is developed. The local PD DAS will exploit Rclone [37] to set up a new cloud storage node, and continuously synchronize the newly detected PD I/Q data and full power-spectrum diagram to the cloud storage at the end of each PD scanning iteration. On the other hand, when the user activates the APP, it will periodically request data synchronization with the cloud server via Google drive API, so that the user can see the updated PD monitoring on their fingertips. In addition, whenever the cloud receives new files, it sends out a notification email to alert the user for newly detected PD events.

3. System Evaluations

3.1. Lab Environment and Hardware Setup

In this section, the system evaluation results are presented. The system has been tested under the lab environment (**Figure 9**), by applying a configurable arbitrary waveform generator (AWG) with a broad bandwidth of 2GHz [38]. The AWG output is connected with a 50 Ω resistive load, which is parallel connected with a 2 G bandwidth oscilloscope [39] with spectrum analyzer to measure the actual signal waveform, amplitude and frequency that is applied onto the resistor. When the AWG signal passes through the resistor, the circuit generates RF signals as a

simulation of PD signals within 100 - 2500 MHz range. Numerical test scenarios have been proceeded, and here we illustrate two representative cases, single-signal and dual-signal detection, to validate the functionalities.

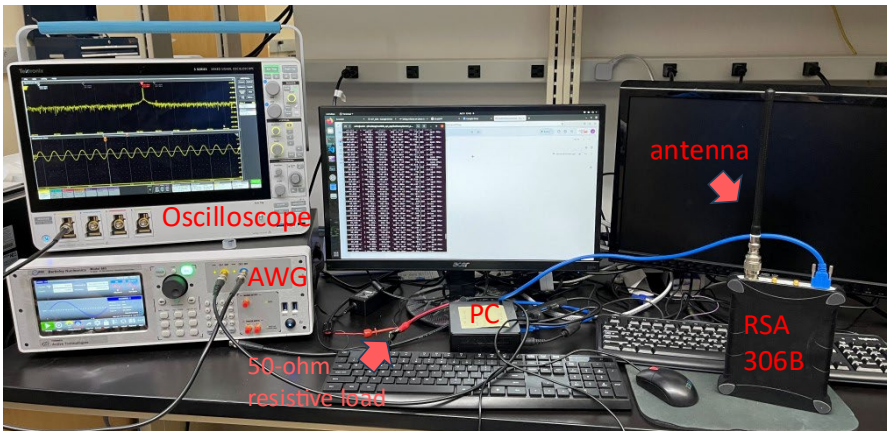

Figure 9. Lab test setup for PD DAS (including antenna, RSA 306B, a portable computer/embedded system), an AWG, a 50-ohm resistor (*i.e.*, PD stimulator), and an oscilloscope.

3.2. Single RF/PD Signal Capturing

We connect the 50 Ω resistor with AWG via BNC-alligator cable, and placed the PD DAS with its antenna about one foot away from the resistor. Once the PD DAS is turned on and initiated with the program to scan RF/PD signals in the air, we set up the AWG to generate a 315 MHz sine waveforms of 1V peak-to-peak. Then, the DAS captures the RF signals that exceed the preset threshold (**Figure 10**), and generates one spreadsheet (*i.e.*, .csv file) of signal value in time-domain (*i.e.*, I/Q ADC values), and a power-spectrum diagram in frequency domain (**Figure 11(a)** and **Figure 11(b)**). In the end of that particular scanning iteration, a complete power-spectrum diagram is drawn from 100 MHz to 2500 MHz (**Figure 11(c)**). Another test results of 768 MHz RF/PD signal are demonstrated in **Figure 11(d)**-(f). One can see that although there exist some relatively low frequency noises, most less than 1 MHz and −60 dB, RF/PD signals of interest can be clearly captured without much interference. In addition, the IF modulation

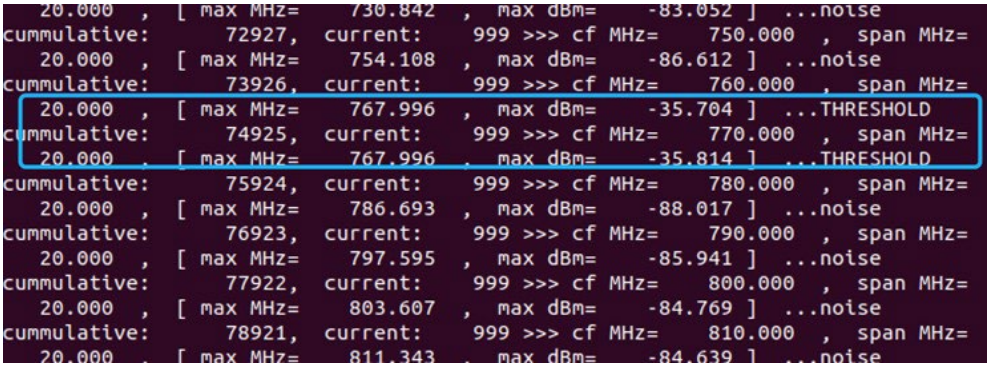

Figure 10. Capturing signals exceeding the power threshold.

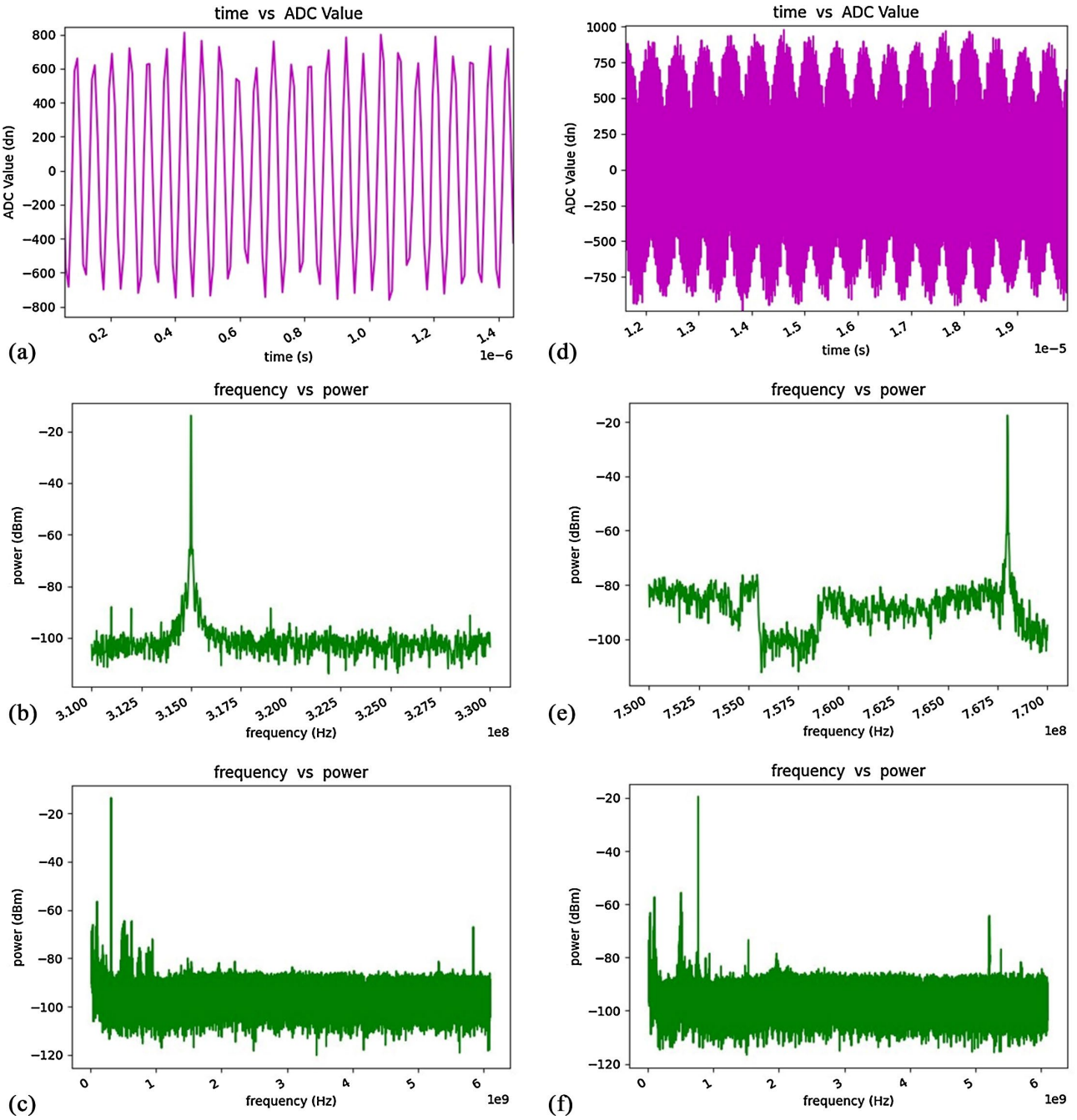

Figure 11. (a) Capturing 315 MHz RF/PD signals with ADC values in time domain; (b) Impulse at 315 MHz in frequency domain for one frame; (c) Impulse at 315 MHz in complete scanning iteration; (d) Capturing 768 MHz RF/PD signals with ADC values in time domain; (e) Impulse at 768 MHz in frequency domain for one frame; (f) Impulse at 768 MHz in complete scanning iteration.

can be observed in **Figure 11(a)** and especially in **Figure 11(d)**, because of the higher IF carrier frequency.

3.3. Dual/Multiple RF/PD Signal Capturing

We also have run the dual RF/PD detection test to confirm that if multiple PD events occur approximately at the same time (*i.e.*, in one scanning iteration), the

PD DAS can capture both of them. We first create a Bluetooth signal (*i.e.*, about 2400 MHz) by turning on two Bluetooth devices and transmitting large files from one device to the other. Meanwhile, we create another 768 MHz signal with AWG as aforementioned, and turn on the PD DAS. It is worth noting that we have to adjust the RF/PD detection threshold to −70 dB so as to catch the low-power Bluetooth signal. As depicted in Figure 12, one can see that the DAS can clearly capture both 768 MHz and the Bluetooth signals.

The confirmation of capturing multiple RF signals of various frequency demonstrates the capability and adaptivity of detecting a variety of PD signals simultaneously. Yet, the power threshold for signal detection needs to be carefully selected as it balances the detection rate and false alarms. Meanwhile, various signal filter techniques (e.g., band-pass and band-stop filters, wavelet filtering, etc.) can be applied to distinguish the hazard PD signals from the routine RF traffic with known spectrums.

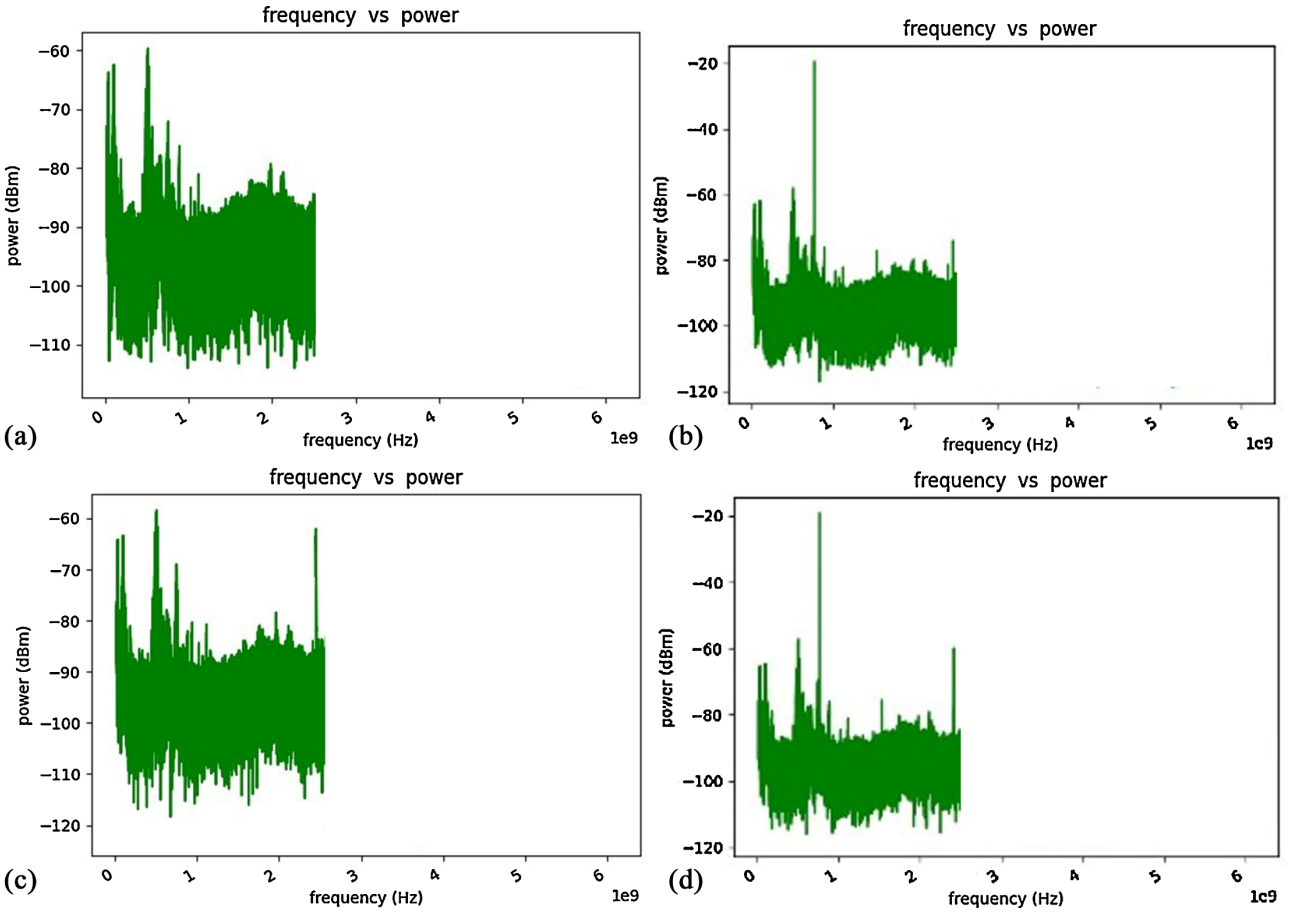

Figure 12. (a) No test signal generated (only noises); (b) Only with a 768 MHz generated by AWG; (c) Only with a Bluetooth signal at about 2400 MHz; (d) With both 768 MHz and Bluetooth signals in the air.

3.4. Cloud-Cased Remote Monitoring

The cloud service is established on the DAS via Google drive and Rclone, so that any files created and edited within this particular Google drive folder will be

automatically synchronized in all terminals that use the same Google drive account. Once the user logs in with proper credentials (Figure 13(a)) on a remote device (e.g., a smartphone), one can see the updated I/Q data and spectrum diagrams (Figure 13(b)), and corresponding file attribute details (Figure 13(c)). In addition to the real-time synchronization from the local PD DAS to the cloud and granting remote accessibility, the cloud also sends a notification email to the user whenever any new PD signals are detected (Figure 13(d)). In that case, personnel who is in charge of monitoring the switchgears and transformers in high-speed

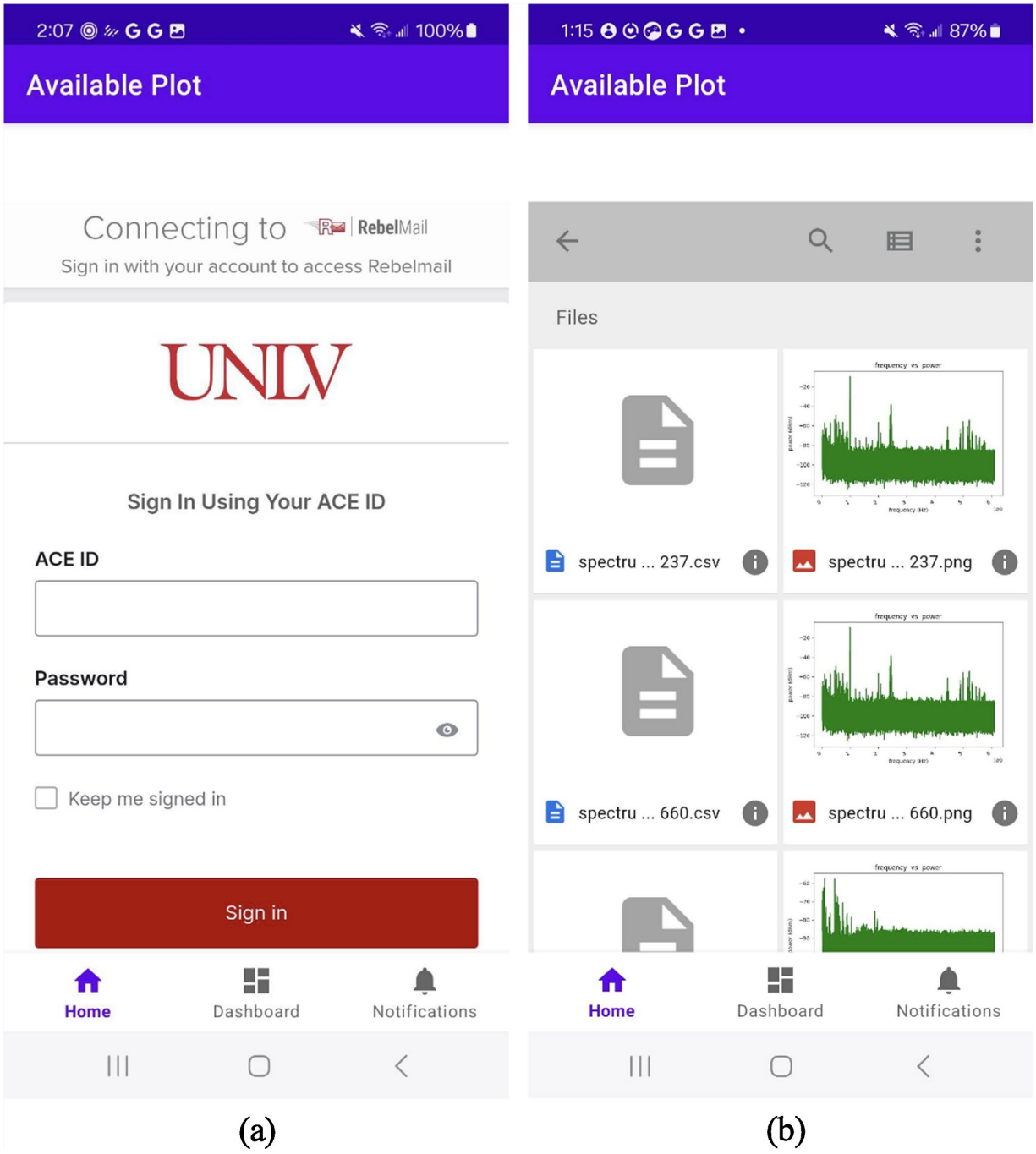

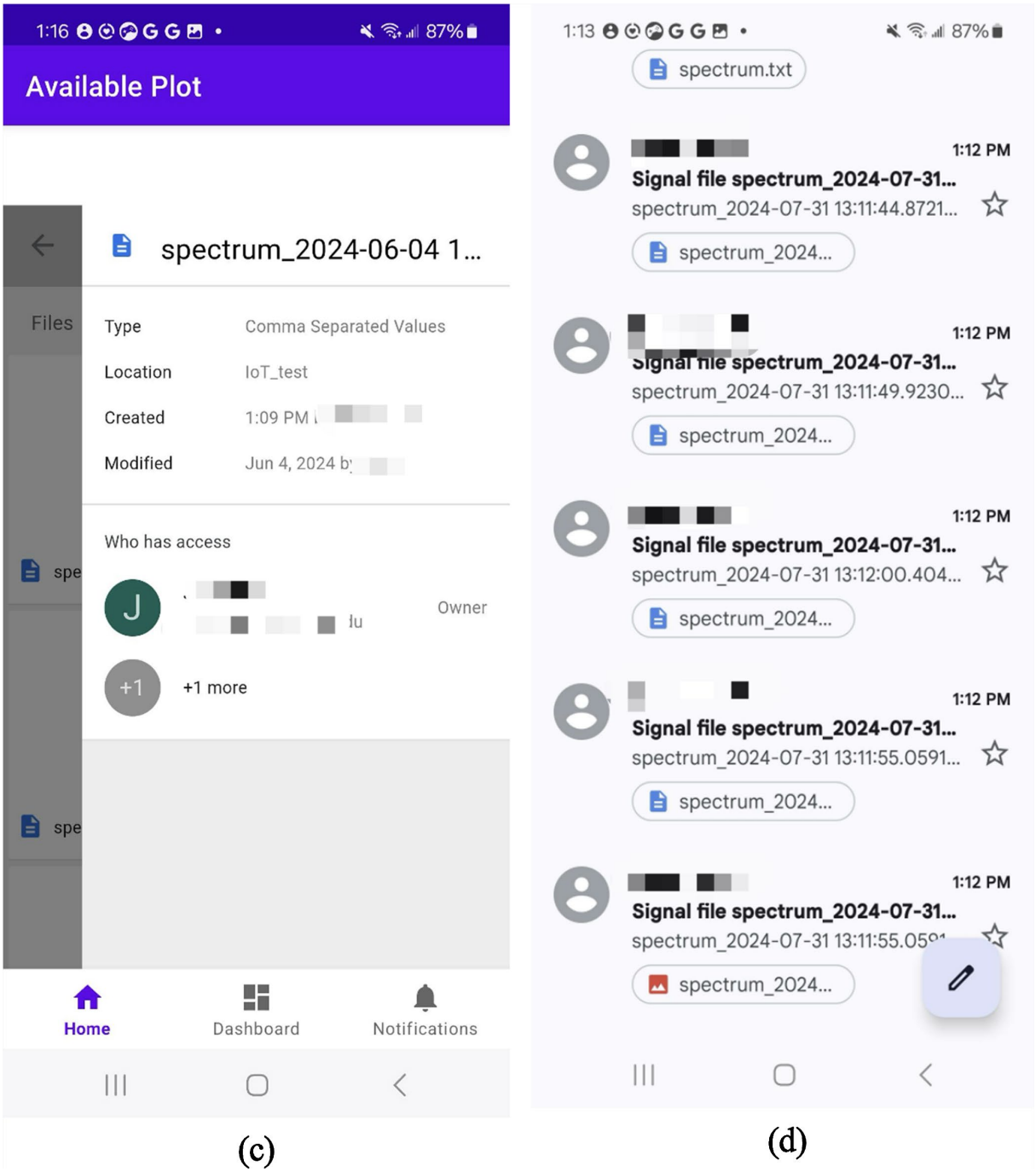

Figure 13. (a) APP login; (b) APP access to files; (c) File attribute details; (d) Email notifications of detected PD events.

rail can be alerted at early stage to minimize the potential damage and maintenance cost PD may cause.

4. Conclusions

This study has successfully developed an advanced platform for the non-disruptive, continuous, real-time detection and monitoring of partial discharges in switchgears and transformers used within high-speed rail infrastructure. The sys-

tem is designed to iteratively scan and capture PD signals within a frequency range of 100 MHz to 2500 MHz, ensuring comprehensive coverage and detection of PD activities.

In addition to its robust detection capabilities, the system is seamlessly integrated with cloud services, enabling remote accessibility to real-time PD data and analysis results. This feature facilitates prompt decision-making and timely interventions by maintenance teams, significantly enhancing the overall reliability and safety of high-speed rail operations.

Extensive laboratory evaluations have been conducted to assess the system's performance. These evaluations demonstrate the system's effectiveness and proficiency in automated real-time PD detection and long-term monitoring. The results indicate that the platform not only meets but exceeds the operational requirements, ensuring that potential faults are identified and addressed promptly before they can escalate into major issues.

The successful implementation of this platform marks a significant advancement in the maintenance and monitoring of high-voltage electrical infrastructure in high-speed rail systems. By leveraging real-time data and remote monitoring capabilities, this system represents a proactive approach to infrastructure management, reducing the risk of unexpected failures and enhancing the overall efficiency and safety of high-speed rail operations.

Acknowledgements

This study was conducted with the support from the USDOT Tier 1 University Transportation Center on Railroad Sustainability and Durability with the grant no. 69A3551747132.

Conflicts of Interest

The authors declare no conflicts of interest regarding the publication of this paper.

References

[1] Givoni, M. (2006) Development and Impact of the Modern High-speed Train: A Review. *Transport Reviews*, **26**, 593-611. https://doi.org/10.1080/01441640600589319

[2] Campos, J. and de Rus, G. (2009) Some Stylized Facts about High-Speed Rail: A Review of HSR Experiences around the World. *Transport Policy*, **16**, 19-28. https://doi.org/10.1016/j.tranpol.2009.02.008

[3] California High-Speed Rail Authority (2008) High-Speed Rail in California. https://hsr.ca.gov/high-speed-rail-in-california/

[4] Sibal, V. (2010) Technical Memorandum: Traction Power Facilities, General Standardization Requirements. California High-Speed Rail Authority.

[5] Douglas, H., Roberts, C., Hillmansen, S. and Schmid, F. (2015) An Assessment of Available Measures to Reduce Traction Energy Use in Railway Networks. *Energy Conversion and Management*, **106**, 1149-1165. https://doi.org/10.1016/j.enconman.2015.10.053

[6] IEC (2014) High-Voltage Switchgear and Controlgear—Part 211: Direct Connection

between Power Transformers and Gas-Insulated Metal-Enclosed Switchgear for Rated Voltages above 52 kV. International Electrotechnical Commission.

[7] Kreuger, F.H. (1989) Partial Discharge Detection in High-Voltage Equipment. Butterworth.

[8] Tenbohlen, S., Beltle, M. and Siegel, M. (2017) PD Monitoring of Power Transformers by UHF Sensors. 2017 *International Symposium on Electrical Insulating Materials* (*ISEIM*), Toyohashi, 11-15 September 2017, 303-306. https://doi.org/10.23919/iseim.2017.8088747

[9] Paoletti, G. and Baier, M. (2001) Failure Contributors of MV Electrical Equipment and Condition Assessment Program Development. *Conference Record of* 2001 *Annual Pulp and Paper Industry Technical Conference* (*Cat. No.*01*CH*37209), Portland, 18-22 June 2001, 37-47. https://doi.org/10.1109/papcon.2001.952946

[10] Davies, N. (2009) Partial Discharge (PD) Techniques for Measuring the Condition of Ageing HV/MV Switchgear. EA Technology International.

[11] Hussain, M.M., Farokhi, S., McMeekin, S.G. and Farzaneh, M. (2016) Prediction of Surface Degradation of Composite Insulators Using PD Measurement in Cold Fog. 2016 *IEEE International Conference on Dielectrics* (*ICD*), Montpellier, 3-7 July 2016, 697-700. https://doi.org/10.1109/icd.2016.7547711

[12] Jahangir, H., Akbari, A., Werle, P. and Szczechowski, J. (2017) Possibility of PD Calibration on Power Transformers Using UHF Probes. *IEEE Transactions on Dielectrics and Electrical Insulation*, **24**, 2968-2976. https://doi.org/10.1109/tdei.2017.006374

[13] Judd, M.D., Li Yang, and Hunter, I.B.B. (2005) Partial Discharge Monitoring of Power Transformers Using UHF Sensors. Part I: Sensors and Signal Interpretation. *IEEE Electrical Insulation Magazine*, **21**, 5-14. https://doi.org/10.1109/mei.2005.1412214

[14] Judd, M.D., Li Yang, and Hunter, I.B.B. (2005) Partial Discharge Monitoring for Power Transformer Using UHF Sensors. Part 2: Field Experience. *IEEE Electrical Insulation Magazine*, **21**, 5-13. https://doi.org/10.1109/mei.2005.1437603

[15] Giussani, R., Cotton, I. and Sloan, R. (2012) Comparison of IEC 60270 and RF Partial Discharge Detection in an Electromagnetic Noise-Free Environment at Differing Pressures. 2012 *IEEE International Symposium on Electrical Insulation*, San Juan, 10-13 June 2012, 127-131. https://doi.org/10.1109/elinsl.2012.6251441

[16] IEEE (2024) IEEE Recommended Practice for Partial Discharge Measurement in Liquid-Filled Power Transformers and Shunt Reactors. IEEE Std C57.113-2023 (Revision of IEEE Std C57.113-2010), 1-45.

[17] Judd, M.D. (2011) Experience with UHF Partial Discharge Detection and Location in Power Transformers. 2011 *Electrical Insulation Conference* (*EIC*), Annapolis, 5-8 June 2011, 201-205. https://doi.org/10.1109/eic.2011.5996146

[18] Timperley, J. (1983) Incipient Fault Identification through Neutral RF Monitoring of Large Rotating Machines. *IEEE Transactions on Power Apparatus and Systems*, **102**, 693-698. https://doi.org/10.1109/tpas.1983.318030

[19] Ma, G., Li, C., Mu, R., Jiang, J. and Luo, Y. (2014) Fiber Bragg Grating Sensor for Hydrogen Detection in Power Transformers. *IEEE Transactions on Dielectrics and Electrical Insulation*, **21**, 380-385. https://doi.org/10.1109/tdei.2014.6740762

[20] Sheng, J., et al. (2004) Study on Gas and Oil Separating Plant Used for Online Monitoring System of Transformer. *Conference Record of the* 2004 *IEEE International Symposium on Electrical Insulation*, Indianapolis, 19-22 September 2004, 93-96.

[21] Skelly, D. (2012) Photo-Acoustic Spectroscopy for Dissolved Gas Analysis: Benefits and Experience. 2012 *IEEE International Conference on Condition Monitoring and Diagnosis*, Bali, 23-27 September 2012, 29-43. https://doi.org/10.1109/cmd.2012.6416446

[22] Sparkman, O.D., et al. (2011) Gas Chromatography and Mass Spectrometry: A Practical Guide. Academic Press.

[23] Kim, D., et al. (2017) A Fiber-Optic Multi-Stress Monitoring System for Power Transformer. 2017 25*th Optical Fiber Sensors Conference* (*OFS*), Jeju, 24-28 April 2017, 1-4.

[24] Kucera, M., Jarina, R., Brncal, P. and Gutten, M. (2019) Visualisation and Measurement of Acoustic Emission from Power Transformers. 2019 12*th International Conference on Measurement*, Smolenice, 27-29 May 2019, 303-306. https://doi.org/10.23919/measurement47340.2019.8779880

[25] Qian, S., Chen, H., Xu, Y. and Su, L. (2018) High Sensitivity Detection of Partial Discharge Acoustic Emission within Power Transformer by Sagnac Fiber Optic Sensor. *IEEE Transactions on Dielectrics and Electrical Insulation*, **25**, 2313-2320. https://doi.org/10.1109/tdei.2018.007131

[26] Fabian, J., Neuwersch, M., Sumereder, C., Muhr, M. and Schwarz, R. (2014) State of the Art and Future Trends of Unconventional Pd-Measurement at Power Transformers. *Journal of Energy and Power Engineering*, **8**, 1093-1098. https://doi.org/10.17265/1934-8975/2014.06.015

[27] Sarkar, B., Koley, C., Roy, N.K. and Kumbhakar, P. (2015) Condition Monitoring of High Voltage Transformers Using Fiber Bragg Grating Sensor. *Measurement*, **74**, 255-267. https://doi.org/10.1016/j.measurement.2015.07.014

[28] Hauschild, W. and Lemke, E. (2019) High-Voltage Test and Measuring Techniques. Springer International Publishing.

[29] Kim, Y. and Hikita, M. (2013) A Proposal for Hybrid PD Sensor Identifying Absolute Distance from PD Source. 2013 *Annual Report Conference on Electrical Insulation and Dielectric Phenomena*, Chenzhen, 20-23 October 2013, 1177-1180. https://doi.org/10.1109/ceidp.2013.6748319

[30] Kraetge, A., Hoek, S., Koch, M. and Koltunowicz, W. (2013) Robust Measurement, Monitoring and Analysis of Partial Discharges in Transformers and Other HV Apparatus. *IEEE Transactions on Dielectrics and Electrical Insulation*, **20**, 2043-2051. https://doi.org/10.1109/tdei.2013.6678852

[31] Luo, Y.F., Xin, X.H., Du, F., Tang, X. and Li, Y.M. (2015) Comparison of DOA Algorithms Applied to Ultrasonic Arrays for PD Location in Oil. *IEEE Sensors Journal*, **15**, 2316-2323. https://doi.org/10.1109/jsen.2014.2374182

[32] Bergmans, J.W.M. (2013) Digital Baseband Transmission and Recording. Springer.

[33] Whitaker, J.C. (2017) The RF Transmission Systems Handbook. CRC Press.

[34] Tektronix, R. (2015) RSA306B USB Real Time RF Spectrum Analyzer. https://www.tek.com/en/products/spectrum-analyzers/rsa306

[35] Tektronix (2017) RSA306, RSA306B, and RSA500A/600A Series Spectrum Analyzers Application Programming Interface (API) Programming Reference. https://www.tek.com/en/spectrum-analyzer/rsa306-manual/rsa306-rsa306b-and-rsa500a-600a-0

[36] Gast, M. (2005) 802.11 Wireless Networks: The Definitive Guide. O'Reilly Media.

[37] Craig-Wood, N. (2014) RCLONE. https://rclone.org/

[38] BNC (2021) Arbitrary Waveform Generator—Model 685. BNC. https://www.berkeleynucleonics.com/model-685

[39] Tektronix (2020) 5 Series B MSO Mixed Signal 8 Channel Oscilloscope. https://www.tek.com/en/products/oscilloscopes/5-series-mso